Vol. 40, No. 3 (2018) 370-391, DOI: 10.24874/ti.2018.40.03.04

Tribology in Industry

www.tribology.rs

RESEARCH

Effect of TiO_2 Nanoparticles Blended with Lubricating Oil on the Tribological Performance of the Journal Bearing

S.R. Suryawanshi[a], J.T. Pattiwar[b]

[a]*Mechanical Engineering Department, MET's IOE, BKC, Nasik, SPPU, Pune, India,*
[b]*SMES SCOE, Nashik, SPPU, Pune, India.*

Keywords:

Plain Journal Bearing
Elliptical Journal Bearing
Titanium dioxide nanoparticles
Coefficient of friction
Wear scar diameter

Corresponding author:

Shubham R. Suryawanshi
Mechanical Engineering Department,
MET's IOE, BKC, Nasik, SPPU,
Pune, India.
E-mail: shubhamsuryawanshi255@gmail.com

A B S T R A C T

This paper presents the performance analysis for plain and elliptical journal bearing operating with industrial lubricants. Titanium dioxide nanoparticle of size 40 nm is used as a lubricant additive to examine the performance of the bearing. Comparative analysis is carried out for three different lubricants with titanium dioxide (0.5% wt) nanoparticles. Performance of bearing is measured at speeds ranging from 500 r.p.m. to 1000 r.p.m. and at 1000 N load. The study of antiwear and antifriction properties for lubricants is carried out on four ball Tribo-tester for operating conditions specified by ASTM standards. An influence of titanium dioxide as an additive on the performance characteristics of the journal bearing such as pressure distribution, load carrying capacity, attitude angle, power loss, oil flow rate, side leakage, frictional force and temperature rise in a film is examined in this paper. The elliptical journal bearing improves the performance of a system over plain bearing operating with the same lubricant.

1. INTRODUCTION

Hydrodynamic bearings are familiar parts of rotating machinery. Journal bearings endow with a cylindrical bearing face on which the shaft running through the bearing lies. The study of journal bearings has concentrated on various features of engineering. The concept of hydrodynamic journal bearing can be found in many areas of the study of stress, material composition, the behavior of the fluid, applied thermodynamics, vibration, and instrumentation. So many researchers are carrying out a research on the stability analysis of the journal bearing system, as it is the crucial area of the dynamics. Nevertheless, the concept of instability created by oil whirl is not intelligible. This needs a clear understanding of the oil whirl and whip phenomenon to identify the valuable fault of a system. The structure of hydrodynamic journal bearing due to this effect is observed as shown in Fig. 1 that is used for the steam turbine in thermal power plant situated at Eklahre, Nashik, India.

Fig. 1. An effect of metal to metal contact due to whirl.

The action of whirl instability may lead of the damage of the system. It decreases the performance of the bearing and affects the lubricant viscosity as it depends on the temperature. The geometry of bearing has a crucial impact on the whirl phenomenon, so it is necessary to analyze the performance characteristics for different geometries of bearing considering thermal effects. Some of the researchers [14,17-19,21,24,27-30,32-46] have provided the study on the thermal effect and an influence of lubricant additives on the performance of the system.

2. LITERATURE REVIEW

Ram et al. [1,9] analyzed the hybrid journal bearing with an iterative method by using FEM. Micropolar lubricant showed better performance than Newtonian lubricant as it influences the minimum film thickness effectively. The pressure in film, bearing flow, coefficient of friction, stiffness and damping coefficient in fluid film and threshold speed were also considered for the analysis. Gertzos et al. [2] carried out the simulation analysis using CFD as a medium. Fluent software is used to solve the equations. Various dimensionless parameters with different L/D ratio were obtained for a Bingham lubricant to carry out comparative analysis. From the study of performance, Bingham lubricant showed better results than Newtonian lubricant as pressure in a film, frictional force, and load carrying capacity increased effectively. Lin et al. [3] Analyzed the different bearings with multi grooves (two, four, five and six) considering the cavitation phenomenon. FSI technique was applied for the iterations. As the load increased, pressure in a film, the temperature in a bearing and eccentricity also increased. The cavitation effect and temperature rise reduced effectively as the number of grooves increased. Deligant et al. [4] have done modelling for journal bearing using CFD as a tool to study an effect of frictional losses which was used in the turbocharger. Simulated results showed good agreement with earlier experimental results as power and torque increased with an increase in the speed of rotation for different inlet oil temperatures. Bompos et al. [5] obtained the results for various parameters by simulating journal bearing with magnetorheological fluid as a lubricant using CFD approach. Eccentricity ratio decreased effectively for L/D ratio between 0.5 to 2, whereas an attitude angle increased. Chasalevris et al. [6] proposed a technique to solve Reynold's equation by an analytical method. Numerical methods were compared by calculating damping as well as stiffness coefficients. Reynold's equation can be solved exactly with the help of analytical method. Brito et al. [7] carried out a comparative analysis by experimental method for journal bearing system with one and two grooves respectively. Flow rate and temperature rise reduced effectively with an increase in load and angle respectively as the number of grooves increased. Papadopoulos et al. [8] identified the clearance in the system with the help of finite element technique. The matrix method was recommended to recover out the stiffness and damping coefficients. It was found that both the coefficients were reduced as the rotational speed was increased for various worn effects in bearing. Dhande and Pande [10] have presented a study based on experimental approach considering cavitation phenomenon. An effect of speed on the cavitation was presented in the range between 1000 to 5000 r.p.m. Multiphase flow was examined to determine the influence of cavitation on the pressure generated in the bearing system. Montazeri [11] focused on his research work based on ferrofluid as a lubricant using numerical and CFD technique. An effect of magnetic field on the performance of bearing system was investigated. It was found that the attitude angle and load carrying capacity increased effectively whereas the coefficient of friction decreased when bearing was operating with ferrofluid as a lubricant. Ouadoud et al. [12] solved a modified Reynold's equation considering micro polar lubricant with respect to cavitation problem. Equations were solved by a numerical

technique using alternating direction implicit (ADI) method. With the help of micro polar lubricant; load carrying capacity and temperature increased while the frictional coefficient and side leakage flow were reduced. Binu et al. [13] designed an experimental setup for journal bearing having twin grooves. The pressures of oil film along the bearing surface were measured with the help of pressure sensors and verified with theoretical pressure values. An experimental analysis was carried using SAE 30 as a lubricant. Experimental maximum pressure was nearly 20% lesser than the theoretical maximum pressure value. Boubendir et al. [14] worked on the thin lubrication system in a journal bearing by solving the equations using CFD technique. Analysis of various L/D ratios was carried out. As the ratio of L/D increased from 0.25 to 2, the pressure increased in a linear manner while wall shear stress and turbulent viscosity decreased apparently. Nicodemus et al. [15] carried their research work on hybrid journal bearing operating with micropolar lubricant. The study on influence of lubricant on stiffness coefficient, film damping coefficient with various recess shapes was represented in this paper. Rahmatabadi et al. [16] also focussed their study using micro polar lubricant. They have solved the basic fundamental equations using generalized differential quadrature (GDQ) method. Performance analysis was carried out for both plain as well as elliptical bearing and concluded that GDQ method can be used as an effective tool rather than other techniques. Garg et al. [17] made a thermohydrostatic analysis of hybrid journal bearing and observed that the temperature distribution values were in excellent agreement with previously published results. The study of the non-Newtonian behavior of lubricant in relation with stiffness and damping coefficients was also presented. Fillon et al. [18] have experimentally performed analysis on journal bearing from steady state to thermal stable state. Temperature and pressure profile plotted across the bearing surface at a wide range of oil flow rate and frictional torque. It was proved that the temperature profile was obtained later than a pressure profile in the bearing due to the cavitation phenomenon. Mongkolwongrojn et al. [19] also have adopted non-Newtonian lubricant for their research. The plain journal bearing was analyzed for various parameters with respect to surface roughness phenomenon. In this work; stiffness and damping coefficients, whirl ratio with roughness amplitude were investigated for different direction with different material. Nair et al. [20] carried out comparative analysis of Newtonian and micro polar lubricants used in the system. They found that, at a maximum eccentricity ratio the stability of a system disturbed for both the lubricants and oil whirl frequency decreased with an addition of some additives. Sharma et al. [21] presented an effect of elastohydrodynamic study on the performance of hole entry hybrid journal bearing using theoretical approach. They summarized that pressure distribution in the film, minimum film thickness, fluid flow, stiffness and damping coefficients increased as the values of deformation coefficient increased from 0 to 5. Ene et al. [22] reported a transient study to analyze the journal bearing having a triple wave geometry. Whirl frequency was tested on a journal bearing system using an FFT analyzer with respect to different operating conditions. From experimental analysis, the system showed less susceptibility up to 60000 r.p.m. That means it is stable up to that speed having an amplitude ratio 0.305. Mishra et al. [23] have studied the different contour plots for temperature in an elliptical (lobed) bearing. From the results it can be summarized that due to elliptical geometry of the bearing the temperature gets reduced and cooling effect also produced. But at the same time pressure distribution hampered to some extent it runs downward. Kuznetsov et al. [24] presented an experimental outcome for the system considering liner deformation using different lining materials. PTFE material was recommended as it provides rise in load carrying capacity, oil film temperature. Brito et al. [25] explained how performance was affected by the feed rate of lubricant in the journal bearing system. They have considered the bearings with one and two grooves for the analysis. With a wide range of speed and load, feeding conditions were analyzed. Twin axial groove bearing showed better results than a single groove bearing. Miranda and Faria [26] have studied different frequency spectrum to analyze the vibration in a bearing system. An elliptical journal bearing was considered for the analysis using FEM technique. The parameters such as amplitude, acceleration were observed for various speeds & obtained frequencies for concern speeds. Wang et al. [27] considered couple stress fluid as a lubricant to carry out thermo hydrodynamic analysis. When

journal bearing operated with couple stress lubricant the load carrying capacity and frictional force increased, whereas the coefficient of friction reduced. It was observed that the side leakage flow remained constant with couple stress lubricant. Sehgal [28] investigated an offset half & elliptical journal bearing considering thermal effects. Analysis was carried out on various grades of oils and speeds to identify the effect on temperature profile, pressure & Sommerfeld number. For various oils, offset half journal bearing showed better performance as load carrying capacity increased & power loss reduced than an elliptical journal bearing. Binu et al. [29] performed a study to determine the performance parameters for circular journal bearing operating with nanofluid having TiO_2 as a nanoparticle additive in the lubricating oil. The viscosity of oil was computed by using Krieger-Dougherty model. An experimental analysis was carried out using SAE 30 as a lubricant. However, the values obtained are using MATLAB code and validated with previously published papers. Baskar et al. [30,32] described an influence of CuO, TiO_2 & WS_2 nanoparticles on the performance of chemically modified rapeseed oil (CMRO). Antiwear and frictional characteristics were analyzed using four ball tester. Amongst selected nanoparticles, CuO nanoparticles as an additive showed better performance as coefficient of friction and wear scar diameter reduced significantly for CMRO lubricant. The amount selected for nanoparticle is 0.5% wt of lubricant. Hu et al. [31] have found that the wear resistance improved by reducing friction with MoS_2 as a lubricant additive. They considered micro as well as nano-structure of MoS_2 for the comparative analysis. These two MoS_2 structures had a synergistic lubrication that influenced the performance. Wan et al. [33] used boron nitride (BN) as a lubricant additive for performance analysis. They have considered SAE 15W40 as a base oil with 0.1%wt, 0.5%wt and 1.0%wt of BN as an additive. After comparative analysis, 0.1% wt as an additive showed higher performance than the other two cases. Frictional coefficient and anti-wear properties were significantly improved using 0.1%wt of BN in a base oil. Charoo and Wani [34] checked the behavior of oil SAE 20W40 using 0.5%wt of IF-MoS_2 as a lubricant additive. The trials were conducted at different loads using ASTM standards on four ball tester. The wear scar diameter reduced by 20 % after addition of IF-MoS_2 and observed coefficient of friction 0.0772 as a minimum value with prepared sample. Ilie and Covaliu [35] improved the solubility of nanoparticles in a base oil to enhance the performance. TiO_2 was used as a nanoparticle of size 50-100 nm to check the dispersion phenomenon. They proposed a new technology for dispersion of nanoparticle in a base oil which improve anti-oxidation, anti-wear and anti-friction properties of oil. Laad and Jatti [36] have used pin on disc tribometer to evaluate tribological properties of oil Servo 4T 10W30 using different concentrations of TiO_2. The tests were carried out at different loads between 4 kg to 6 kg. The frictional coefficient was significantly scaled down by 86 % at 4 kg load for 0.3%wt of TiO_2. The performance characteristics such as anti wear and anti friction properties improved for an engine oil operating with TiO_2. Ali et al. [37-39] proposed the hybrid lubricant containing Al_2O_3 and TiO_2 nanoparticles in the piston ring/cylinder liner contact. The scuffing resistance was improved after implementing the hybrid nanolubricant. The frictional power losses were reduced by 40-51 % and wear rate decreased by 17 % using hybrid nanolubricant that would have promising approach to automotive fuel economy and an increased life span for engine parts. Gunnuang et al. [40] analyzed the performance of journal bearing using Al_2O_3 nanoparticles. Carreau viscosity model was implemented in the study for multigrade engine oil SAE 10W50. Results revealed that the load carrying capacity increased after addition of Al_2O_3 nanoparticles but the film temperature remained almost same. Solghar [41] have also taken Al_2O_3 as a lubricant additive in the base oil. The coefficient of friction and load carrying capacity were increased whereas flow rate was decreased after addition of Al_2O_3 nanoparticles. Shenoy et al. [42] considered API-SF engine oil blended with three different nanoparicles such as nano-diamond, titanium dioxide (TiO_2) and copper oxide (CuO) to analyze the performance of the fluid film journal bearing. Out of three nanoparticle additives, TiO_2 showed the best performance for static characteristics. The load carrying capacity and friction increased while end leakage was decreased significantly for journal bearing. Nicoletti [43] investigated the thermal properties and static characteristics of hydrodynamic journal bearing operating with

nanolubricants. Six various nanoparticles Si, SiO_2, Al, Al_2O_3, Cu and CuO were taken in the study with ISO VG 68 as a base fluid. It was observed that the volumetric heat capacity was increased with the addition of nanoparticles in the base fluid. Amongst six nanoparticles, the lubricant containing CuO nanoparticles showed better results to achieve higher volumetric heat capacity. Azmi et al. [44] proposed the conversion of nanofluid weight concentration into volume concentration with equations. They considered SiO_2 nanofluid with 99.99 % purity and used in the experiments after appropriate dilution. Khuong et al. [45] implemented four ball tester to identify the performance of engine oil blended with bioethanol-gasoline. An impact of bioethanol-gasoline on the wear and frictional properties was discussed at various operating conditions. Babu et al. [46] performed a study on an engine oil SAE 15W40 in addition with Al_2O_3 and ZnO as a nanoparticle. Authors have presented a mathematical moel based on viscosity-temperature relation. With the addition of 0.5%wt of nanoparticle, the performance parameters were evaluated. Load carrying capacity and frictional force increased for eccentricity ratio of 0.9.

A thorough study of the literature based on journal bearing configurations and lubricant additives reveals that very few researchers have focussed on the non-circular journal bearings operating with nanoparticle additives. Thus, this research work is aimed to bridge the gap in the literature by considering the circular and elliptical geometry of the bearing operating with TiO_2 nanoparticle as an additive. An elliptical bearing is selected for non-circular geometry as it decreases the oil whirl, improves the damping capabilities and is an ease to manufacture than other bearing configurations [25]. The performance characteristics of the plain and elliptical journal bearing operating with three lubricants are investigated analytically. To implement the nanolubricant in the analytical approach, the properties of nanolubricant are investigated on four ball tribo-tester. The viscosity of the three grades of lubricants with the addition of TiO_2 nanoparticle of size 40 nm (0.5%wt) is computed using modified Krieger Dougherty model and is validated by using Redwood Viscometer.

3. THEORETICAL ASPECTS

A lubrication theory initially is proposed by Navier, Stokes and they have given a solution to the basic equations. Later Reynold extended the work, and derived an equation known as Reynold's equation, which is popularly applicable and accepted in most of the hydrodynamic theories. The key parameters considered to achieve an equation are viscosity, density, and film thickness of a lubricant.

The following assumptions have been considered during the study [48]:

i. The lubricant is incompressible.
ii. The inertia forces in the oil film are negligible.
iii. The viscosity of the lubricant is constant.
iv. The effect of curvature of the film with respect to film thickness is neglected.
v. The shaft and bearing are rigid.
vi. There is continuous supply of lubricant.
vii. There is no slip at the boundaries.
viii. The flow is laminar.

3.1 Pressure distribution in an oil film

Reynolds's equation in two dimensional form is known as [1,9,10,15,21,47,48],

$$\frac{U}{2}\frac{\partial h}{\partial x}-\frac{1}{12\mu}\frac{\partial}{\partial x}\left(h^3\frac{\partial p}{\partial x}\right)-\frac{1}{12\mu}\frac{\partial}{\partial z}\left(h^3\frac{\partial p}{\partial z}\right)=0 \quad (1)$$

$$\frac{\partial}{\partial x}\left(h^3\frac{\partial p}{\partial x}\right)+\frac{\partial}{\partial z}\left(h^3\frac{\partial p}{\partial z}\right)=6\mu U\frac{\partial h}{\partial x} \quad (2)$$

Now, implying no variation of pressure in the z-direction, the (∂p/∂z) term in the two dimensions is dropped. The governing equation becomes:

$$\frac{\partial}{\partial x}\left(h^3\frac{\partial p}{\partial x}\right)=6\mu U\frac{\partial h}{\partial x} \quad (3)$$

Using polar coordinates x = R .θ and dx = R dθ; Eq. (3) becomes:

$$\frac{\partial}{\partial \theta}\left(h^3\frac{\partial p}{\partial \theta}\right)=6\mu UR\frac{\partial h}{\partial \theta}$$

where:

$$h=C(1+\varepsilon\cos\theta)$$

Applying the boundary pressures as follows, an equation can be derived in polar form as:

i) p = 0 at θ = 0 (γ = 0) and ii) p = 0 at θ = 2π

The second condition of equation is known as full Sommerfeld boundary condition. It indicates the film is full, that is upto 2π. The boundaries θ=0 and θ=2π will transform into the same boundaries which reverted to θ coordinate as:

$$p = \frac{6\mu URe}{C^2}\frac{(2+\varepsilon\cos\theta)\sin\theta}{(2+\varepsilon^2)(1+\varepsilon\cos\theta)^2} \quad (4)$$

3.2 Load Carrying Capacity for Hydrodynamic Journal bearing

The load carrying capacity of hydrodynamic journal bearing is expressed as W and its components W_x and W_y along X and Y directions respectively are shown in Fig. 2.

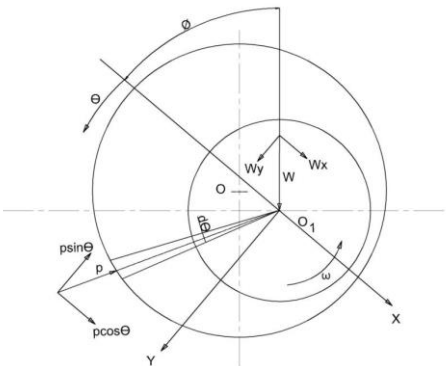

Fig. 2. Components of hydrodynamic force.

The component W_x is indicated along O-O_1. We can write the small component of W having its angular deflection dθ as [47]:

$$dW = p.L.R.d\theta \quad (5)$$

dW_x and dW_Y are the components of dW along the directions of X and Y respectively. It is very convenient to integrate these two components to obtain each component. These components can be writtens as :

$$dW_x = -p.L.R.\cos\theta.d\theta \quad (6)$$

$$dW_y = p.L.R.\sin\theta.d\theta \quad (7)$$

The negative sign in Eq. (6), is due to opposite directions of force components. Integrating the above equations as :

$$W_x = -L.R.\int_0^{2\pi} p.\cos\theta.d\theta \quad (8)$$

$$W_y = L.R.\int_0^{2\pi} p.\sin\theta.d\theta \quad (9)$$

The attitude angle Φ is obtained by the following equation:

$$\tan\phi = \frac{W_y}{W_x} \quad (10)$$

3.3 Impact of Sommerfeld conditions on load capacity

As mentioned in section 3.2, the components of load capacity W_x and W_y are obtained by integration as follows [47,48]:

$$\int p.\cos\theta.d\theta = p.\sin\theta - \int \frac{dp}{d\theta}.\sin\theta.d\theta \quad (11)$$

$$\int p.\sin\theta.d\theta = -p.\cos\theta + \int \frac{dp}{d\theta}.\cos\theta.d\theta \quad (12)$$

By using pressure gradient, equations (11) and (12) can be solved. Integrating the above equations, the value of W_x becomes zero and W_y is obtained as follows:

$$W_y = \frac{6\mu URL^2}{C^2}(I_2 - \frac{h_m}{C}I_3) \quad (13)$$

Where, I_2 and I_3 are defined as:

$$I_2 = \frac{\gamma - \varepsilon\sin\gamma}{(1-\varepsilon^2)^{3/2}}$$

$$I_3 = \frac{1}{(1-\varepsilon^2)^{5/2}}\left[\ \gamma - 2\varepsilon\sin\gamma + \frac{\varepsilon^2}{2}\gamma + \frac{\varepsilon^2}{4}\sin 2\gamma\ \right]$$

Solving the Eq. (13) using above values, equation can be simplified as :

$$W = \frac{12\pi\mu UR^2L}{C^2}.\frac{\in}{\left(2+\in^2\right)\left(1-\in^2\right)^{1/2}} \quad (14)$$

3.4 Friction in a Journal Bearing

The frictional force in the journal bearing is resistance to the shaft rotation due to a viscous fluid film in the bearing. It is defined as [47,48] :

$$F_f = \frac{T_f}{R} \quad (15)$$

The shear stress is defined using following equation considering velocity gradient along Y direction as :

$$\tau_w = \mu\left(\frac{dU}{dy}\right)_{(y=h)} \tag{16}$$

The frictional force is calculated by:

$$F_f = \int_A \tau_{(y=h)} dA \tag{17}$$

After substitution as $dA = R.L.d\theta$ in Eq. (17), the frictional force becomes :

$$F_f = \mu RL \int_0^{2\pi} \tau_{(y=h)} d\theta \tag{18}$$

Putting the value of the shear stress in Eq. (18):

$$F_f = \mu URL \int_0^{2\pi} \left(\frac{4}{h} - \frac{3h_0}{h^2}\right) d\theta \tag{19}$$

The equation (19) is simplified as :

$$F_f = \frac{\mu URL}{C} \frac{4\pi\left(1+2\in^2\right)}{\left(2+\in^2\right)\left(1-\in^2\right)^{1/2}} \tag{20}$$

The frictional coefficient is obtained as follows :

$$f = \frac{F_f}{W} \tag{21}$$

3.5 Power loss

The power loss is defined as follows [47] :

$$P_f = T_f \omega = F_f U \tag{22}$$

Putting an expression of F_f from Eq. (20), the power loss is expressed as :

$$P_f = \frac{\mu U^2 RL}{C} \frac{4\pi\left(1+2\in^2\right)}{\left(2+\in^2\right)\left(1-\in^2\right)^{1/2}} \tag{23}$$

The power loss or energy loss is estimated using the Eq. (23) to identify the heat dissipated in the journal bearing.

3.6 Temperature rise in a fluid film

For design purpose, it is sufficient to estimate the temperature rise of the fluid ΔT. This estimation is based on the simplified assumption that it is possible to neglect the heat conduction through the bearing material in comparison to the heat removed from the continuous replacement of fluid. The following equation is used to compute the temperature rise of oil in a journal bearing [47] :

$$\Delta T = \frac{8.3P\left(\frac{fR}{C}\right)}{10^6\left(\frac{Q}{nRCL}\right)\left(1-0.5\frac{Q_s}{Q}\right)} \tag{24}$$

3.7 Equations for Elliptical bearing

The elliptical journal bearing consisting of two lobes is represented in Fig. 3. The attitude angles for upper lobe and lower lobe are denoted by ϕ_1 and ϕ_2 respectively. The change in the design procedure for an elliptical journal bearing as far as geometry is as follows:

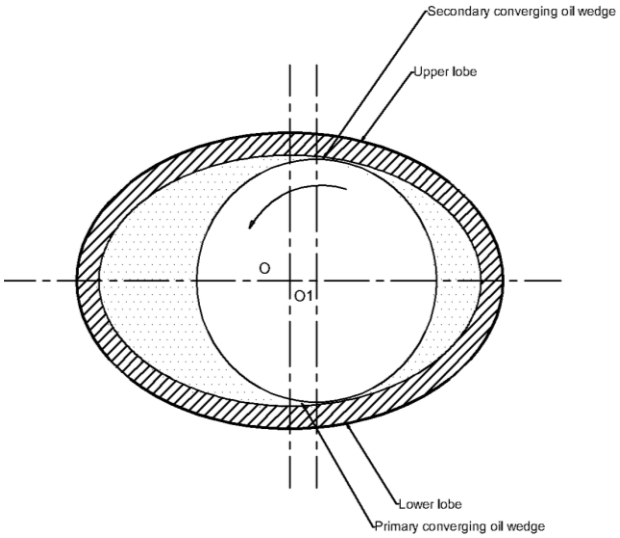

Fig. 3. Geometry of elliptical journal bearing.

Oil film thickness is computed as [28]:

$$h = C_m[1 + E_m + \varepsilon_1 \cos(\theta + \phi - \phi_1)] \quad \text{for } 0° \le \theta \le 180° \tag{25}$$

$$h = C_m[1 + E_m + \varepsilon_2 \cos(\theta + \phi - \phi_2)] \quad \text{for } 180° \le \theta \le 360° \tag{26}$$

where, Eccentricity at upper lobe:

$$\in_1 = [E_m{}^2 + \in^2 - 2E_m.\in.\cos(\phi)]^{1/2} \tag{27}$$

Eccentricity at lower lobe:

$$\in_2 = [E_m{}^2 + \in^2 + 2E_m.\in.\cos(\phi)]^{1/2} \tag{28}$$

$$\phi_1 = \pi - \tan^{-1}\left[\frac{\phi}{E_m - \in.\cos\phi}\right] \tag{29}$$

$$\phi_2 = \tan^{-1}\left[\frac{\phi}{E_m + \in.\cos\phi}\right] \tag{30}$$

Elliptical ratio:

$$E_m = \frac{C_h - C_m}{C_m} \tag{31}$$

Table 1. Geometrical and operating parameters for bearing.

Parameters	Values
Diameter of Journal, D	50 mm
Length of bearing, L	50 mm
L/D Ratio	1
Clearance, C	0.05 mm
Type of Lubricant	MOBIL grade(DTE 24, DTE 25,DTE 26)
Speed of Journal, N	500 -1000 r.p.m.
Load on Journal bearing, W	1000 N
Clearance Ratio, C/R	0.002
Major diameter of elliptical bearing	50.3 mm
Minor diameter of elliptical bearing	50.2 mm
Elliptical ratio, E_m	0.5

The performance analysis for the elliptical bearing is evaluated based on its geometry. Eccentricity ratio, attitude angle, Sommerfeld number is calculated for upper and lower lobe to evaluate the performance parameters mentioned in the Eq.s (27-30) respectively. However, in section 6, the values are selected for the lower lobe region due to a loaded segment of bearing in [10]. The operating conditions and geometrical parameters for bearings are enlisted in Table 1.

4. EXPERIMENTAL DETAILS

The samples of nanolubricant are prepared with the help of overhead stirrer. TiO_2 nanoparticles have been considered as a lubricant additive and physic-chemical properties of lubricating oils have been elaborated in this section. The tribological properties of prepared lubricating samples are examined using four ball tester.

4.1 Preparation of Sample

The TiO_2 nanoparticles purchased by Nanolabs Limited, Jamshedpur, India are added to the lubricating oil at 0.5% wt. The TiO_2 nanoparticles as an additive (0.5% wt) added to the lubricating oil as these nanoparticles are synthetically steady. Hence, the chances of a reaction with base liquid and tribo-surfaces are very less. TiO_2 nanoparticles are effortlessly accessible and safe for human handling. These nanoparticles tends to repress the bacterial development and avert advance arrangement of cell structure [36,37-39]. The morphology of TiO_2 nanoparticles is studied as shown in Fig. 4. The Scanning Electron Microscope (SEM), Ultra-Violet visible spectroscopy (UV) and X-Ray Diffraction (XRD) analyses of TiO_2 nanoparticles are shown in Figs. 4a, 4b and 4c respectively. Figure 4a exhibits that the TiO_2 nanoparticles are whitish in colour and are spherical in crystallographic structure with size distribution in the average range of 30-50 nm. It is also found that the oil additive can keep TiO_2 nanoparticles from agglomeration. Figure 4b represents that spectrum peak is observed at 400 nm wavelength and lowers down effectively as wavelength increases from 400 to 600 nm.

The XRD pattern of TiO_2 nanoparticles reveals that the peaks are observed approximately at 2θ=28.4°, 36.7°, 42.5°, 48°, 54.4°, 63.5°, and 84° with three major strong diffraction peaks at 28.4°, 36.7° and 54.4° indicates spherical structure of prepared sample. With the help of indexed peaks, it is confirmed that TiO_2 nanoparticles are in the anatase structure phase. The results indicate that the structure of TiO_2 nanoparticles remains unchanged after functionalization.

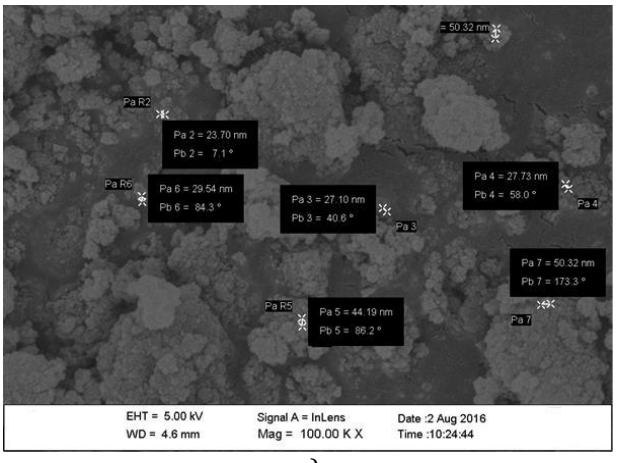

a)

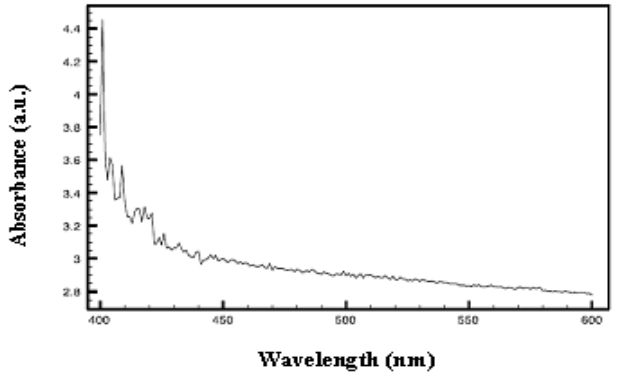

b)

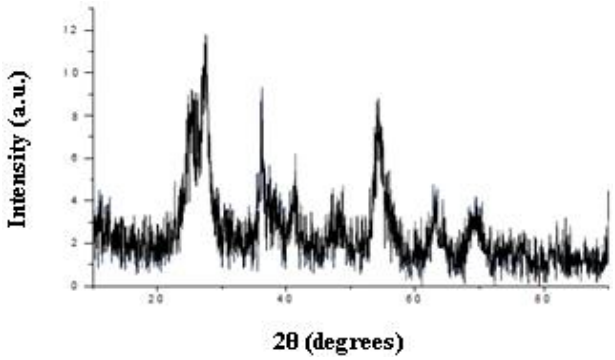

c)

Fig. 4. TiO_2 nanoparticles a) SEM analysis; b) UV spectrophotometer analysis and c) XRD analysis.

Further, compare to other nanoparticle additives TiO_2 nanoparticles are having less density, less molar mass, higher melting point, higher boiling point [49,50]. An overhead stirrer is used for the mixing of TiO_2 nanoparticle of size 40 nm in the base lubricating oil as shown in Fig. 5. The speed for the mixing was kept at 1500 rpm. The requisite amount of nanoparticles is accurately weighed using a precision electronic balance and mixed with the lubricating oil. To achieve proper dispersion of nanoparticles, the sample is placed on magnetic base and a magnetic strip is immersed in the sample to provide magnetization effect. Magnetic strip rotates at 1200 rpm. using the application of voltage in magnetic base. The time of agitation is kept for 30 min in order to devise a stable suspension. The oleic acid is used as a surfactant that modulates the available surface energy of the particles so that the surface tension decreases, allowing more particles to escape the aggregation process.

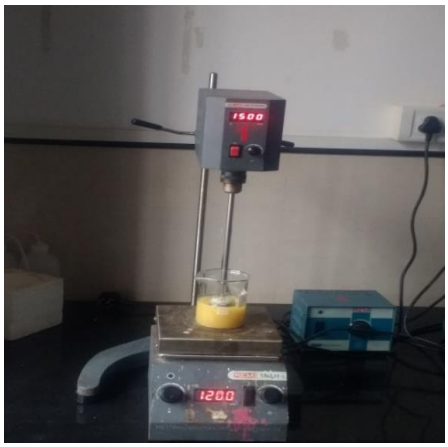

Fig. 5. Stirrer with magnetic effect.

The chemical, physical and thermal properties of TiO_2 are listed in Table 2.

Table 2. Various properties of TiO_2 nanoparticles.

Parameter	Value
Size	40 nm
Size range	30-50 nm
Chemical Composition	Titanium 59.93 % and Oxygen 40.07 %
Density	4.23 g/cm^3
Molar Mass	79.9378 g/mol
Melting Point	1,843 ° C
Boiling Point	2,972 ° C

The light transmittance effect is considered to study the dispersibility of TiO_2 nanoparticles in the base lubricant. The lubricant containing TiO_2 showed better light transmission than the base lubricant without TiO_2 nanoparticles. Even though after a period of six months, there were no sediments found in the nanolubricant.

4.2 Properties of lubricant

The MOBIL DTE 20 series oils (DTE 24, DTE 25, and DTE 26) offer superior oxidation resistance. This property tends to extend the intervals for the replacement of oil and filter. Now a days, the equipment manufacturers are preferring to these oils as they provide exceptional characteristics within a single product. These oils find the applications where hydraulic system plays a vital role. These oils are used in the system where load carrying capacity is high and anti-wear protection as well as thin oil film protection is required. Based on these properties DTE 24, DTE 25 and DTE 26 oils are considered in this study to investigate the performance of journal bearing system. The viscosity of nanolubricant is computed by using modified Krieger-Dougherty viscosity model as per Eq. (45) [29]. The weight concentration of the nanoparticle is converted into the volume concentration by using an Eq. (42) explained below [44]:

$$W_{TiO_2} = \left(\frac{\phi'}{100-\phi'}\right).\left(\frac{\rho_{TiO_2}}{\rho_{bf}}\right).\left(W_{bf}\right) \tag{32}$$

$$\phi' = \frac{\left(\frac{W_{TiO_2}}{\rho_{TiO_2}}\right)}{\left(\frac{W_{TiO_2}}{\rho_{TiO_2}}+\frac{W_{bf}}{\rho_{bf}}\right)} * 100 \tag{33}$$

The Krieger-Dougherty viscosity model is given by:

$$\frac{\mu_{ps}}{\mu_{bf}} = \left(1 - \frac{\phi_a}{\phi_m}\right)^{-2.5\phi_m} \quad (34)$$

where:

$$\phi_a = \phi' \left(\frac{a_a}{a}\right)^{3-D} \quad (35)$$

Furthermore, Eq. (34) is expressed as [44]:

$$\frac{\mu_{ps}}{\mu_{bf}} = \left(1 - \frac{\phi'}{0.5}\left(\frac{a_a}{a}\right)^{1.3}\right)^{-1.25} \quad (36)$$

The viscosity of three grades of lubricant is measured with the help of Redwood Viscometer with a number of trials & average time is taken for viscosity calculations as shown in Table 3.

Table 3. Properties of lubricant.

Lubricant properties	DTE 24	DTE 25	DTE 26
Viscosity, cSt @ 40°C (without nanoparticle)	32.42	46.33	67.43
Viscosity, cSt @ 40°C (with nanoparticle)	33.77	47.13	68.74
Pour Point, °C, ASTM D97	-27	-27	-21
Flash Point, COC, ASTM D92	220	232	236
Relative density/Specific gravity	0.869	0.877	0.885
Density, kg/m^3	869	877	885
Specific heat at constant pressure, J/kgC	1951.0	1942.6	1934.3

4.3 Four ball tester

Four Ball Tester TR-30L model is a versatile equipment combining the feature of both four ball extreme pressure and four balls wear test machine. The properties of lubricant are studied with the help of four ball tester. The three balls are introduced in the lubricant for which friction, wear and extreme pressure test can be carried out. As per the ASTM D 4172 standard, the operating conditions such as speed, temperature, duration and load are set. The wear scar for three balls is measured with the aid of optical microscope having magnification 100x upto 1 mm scar diameter and 40x for 1 mm to 4 mm scar diameter. The frictional torque and wear scar diameter are obtained on computer through data acquisition and image acquisition system respectively using LabVIEW based Winducom software. The selection of proper materials and matching process of the mechanical components ensure a high degree of accuracy and smooth operation of all moving/rotating components with minimum vibrations and noise levels. This tester is used to determine the load carrying, coefficient of friction and anti-wear properties of lubricating oil and greases. It is compatible for both ASTM and IP standards. In this tester machine three 12.7 mm diameter steel balls are clamped together and covered with lubricant to be evaluated. A fourth ball of same diameter referred to as top ball is held in a special collet inside the spindle, rotated by an AC motor. A rotating steel ball is pressed against three steel balls firmly held together and immersed in lubricant under test. The test load, duration, temperature and rotational speed are set in accordance with standard test schedule. In Wear Preventive (WP) tests – also called Anti Wear (AW) tests – the average scar diameter on the bottom three balls is reported.

Fig. 6. Four ball tester machine.

The size of the scar shows the ability of the lubricant to prevent wear. A larger diameter indicates poor wear preventive property while a smaller indicates superior wear preventive property.

Fig. 7. Ball pot.

Additional provision to heat and control temperature of oil sample is also provided at bottom of ball pot which is shown in Fig. 7. Normal load is applied on the balls by loading lever and dead weights placed on loading pan. The ball pot is supported above the loading lever on a thrust bearing and plunger. Beneath plunger, a load cell is fixed to lever to measure the normal load. The frictional torque exerted on three balls is measured by frictional force load cell. The tester unit consisting of a cylindrical main body is mounted over the base plate. Inside at corner of the body, spindle assembly is mounted to rotate the fourth ball. The spindle is driven by an AC motor through a flat belt drive. The AC motor is mounted on the rear portion of an outer body with a flat crowned pulled fixed on its shaft. The pulley height is leveled with spindle pulled height to prevent belt slipping. The pulley ratio is maintained at 1:1 for speeds up to 3000 rpm. An idler pulley is fixed between pulleys to increase the belt tension. The belt drive is covered by a guard for safety. Beneath motor an electric cabinet is fixed to the outer body. Inside it; variable frequency drive (VFD), line filter, transformer and many other electrical items are mounted. The Spindle housing is firmly fixed on the body in vertical direction, so that the fourth ball can be inserted into it from the bottom. The spindle is mounted between two high precision ball bearings inside the housing to take the maximum load and speed without heating and also to rotate with no run out. Up and down movement of the plunger is given by loading lever fixed beneath the plunger to give 1:15 loading ratio. A load cell mounted inside the loading lever has a roller fixed at loading point lifting the plunger resting on it while loading arm is pulled down. The loading pan is suspended at the longer end of the lever arm to place dead weight for applying normal load.

5. RESULTS AND DISCUSSION

The frictional and wear behavior of lubricating samples is presented in this section. The frictional torque is recorded on the computer through data acquisition system. Later, the coefficient of friction is computed from frictional torque using eq. (37). Wear scar diameters of lower three balls are measured before removing from the cup. The coefficient of friction results are based on the average measurement of frictional force measured.

5.1 Measurement of frictional coefficient and wear scar diameter

The anti-friction and anti-wear tests are carried out on four ball tester as per ASTM D 4172 standard. The tests are conducted at 148 N load, 1200 rpm. and 75 ˚C [30]. Each test is carried out for one hour duration as per the specified duration. Three sets have been taken for each test for the sake of repeatability and average reading is considered for further analysis. The mean value of scar diameter is considered for each trial. The analysis is carried out for three grades of lubricants namely MOBIL DTE 24, MOBIL DTE 25 and MOBIL DTE 26. The TiO_2 nanoparticles are added to investigate the friction and wear properties of lubricant. The frictional torque and wear scar diameter are measured for particular three grades of lubricant with and without nanoparticles as shown in Figs. 8-10. The values are stored and the plot of frictional torque with time is plotted in MATLAB. It is found that the coefficient of friction obtained for oil DTE 24 operating without TiO_2 nanoparticles and oil DTE 24 containing TiO_2 nanoparticles is 0.08759 and 0.08228 respectively (Figs. 8a and 8c). The elliptical surface is the wear surface that is studied with the help of the image acquisition system. The mean diameters of these elliptical surfaces for DTE 24 without TiO_2 are 187 μm, 205 μm, 221 μm and for DTE 24 with TiO_2 are 203 μm, 204 μm and 195 μm respectively (Figs. 8b and 8d).

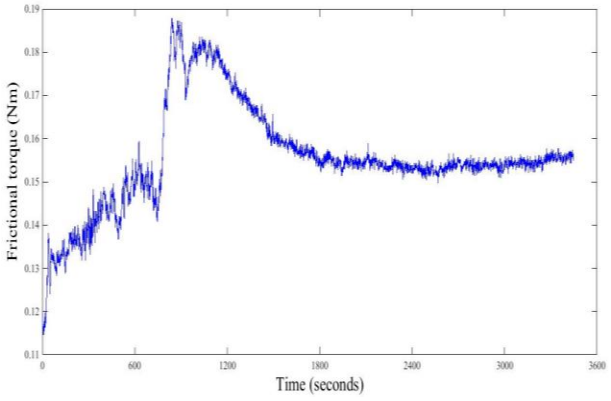

a)

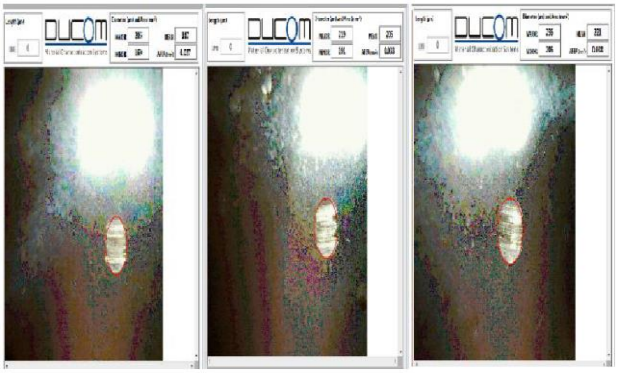

b)

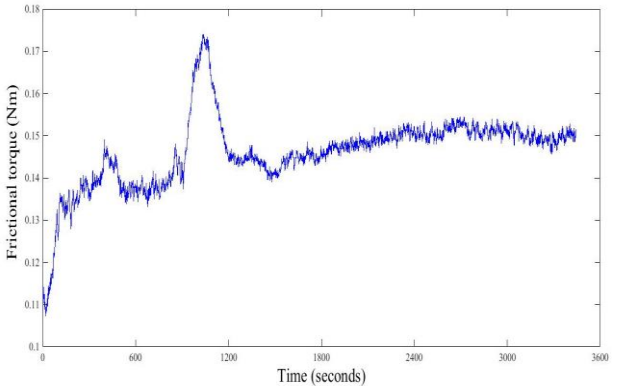

c)

d)

Fig. 8. Friction and wear behavior of MOBIL DTE 24 lubricant: a) Frictional torque without TiO_2 nanoparticles; b) Wear scar view of three balls without TiO_2 nanoparticles; c) Frictional torque with TiO_2 nanoparticles; and d) Wear scar view of three balls with TiO_2 nanoparticles.

The coefficient of friction obtained for oil DTE 25 operating without TiO_2 nanoparticles and oil DTE 25 containing TiO_2 nanoparticles is 0.10414 and 0.09324 respectively (Figs. 9a and 9c). The mean diameters of the elliptical surfaces for DTE 25 without TiO_2 are 209 μm, 219 μm, 184 μm and for DTE 25 with TiO_2 are 184 μm, 188 μm and 196 μm respectively (Figs. 9b and 9d). Similarly, the coefficient of friction obtained for oil DTE 26 operating without TiO_2 nanoparticles and oil DTE 26 containing TiO_2 nanoparticles is 0.08181 and 0.06024 respectively (Figs. 10a and 10c). The mean diameters of the elliptical surfaces for DTE 26 without TiO_2 are 192 μm, 185 μm, 206 μm and for DTE 26 with TiO_2 are 202 μm, 176 μm and 190 μm respectively (Figs. 10b and 10d). The pick values in Figs. 8-10 are observed due to the static friction between the lubricant and the steel balls. The coefficient of friction at this point is very low, resulting into maximum friction at the instant [37-39]. After this phase, the linear phenomenon of curve observed during the test. As per the procedure specified by ASTM D 4172, the mean value of frictional torque is considered for the analysis and coefficient of friction is computed for the same. The profiles of frictional behavior are similar to the work of Baskar et al. [30,32]. The frictional coefficient for balls in contact with the lubricant is computed using the following expression [45]:

$$\mu_b = \frac{T_f \times \sqrt{6}}{3 \times W_b \times r} \tag{37}$$

where T_f, W_b, and r can be expressed as frictional torque (N), applied load on balls (N) and distance measured from the center of the lower ball contact surface to the rotating axis (m), respectively.

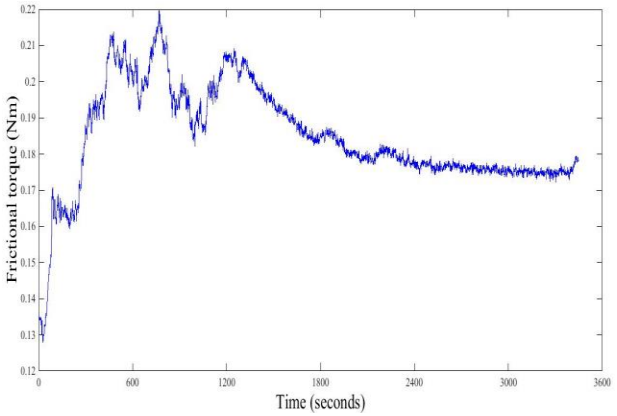

a)

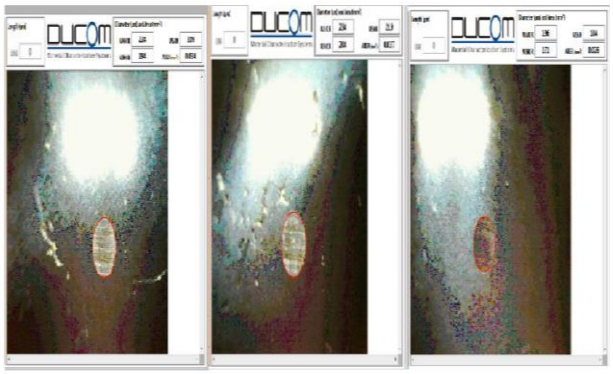

b)

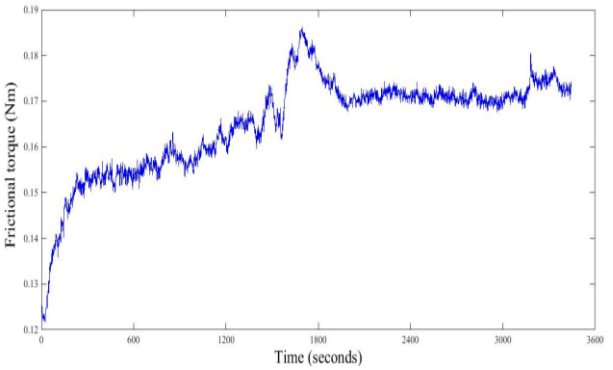

c)

d)

Fig. 9. Friction and wear behavior of MOBIL DTE 25 lubricant: a) Frictional torque without TiO_2 nanoparticles; b) Wear scar view of three balls without TiO_2 nanoparticles; c) Frictional torque with TiO_2 nanoparticles; d) Wear scar view of three balls with TiO_2 nanoparticles.

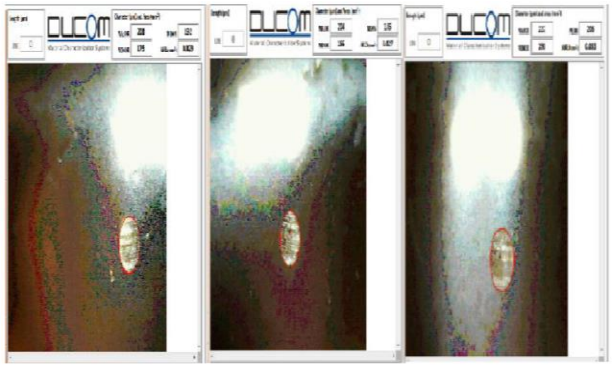

b)

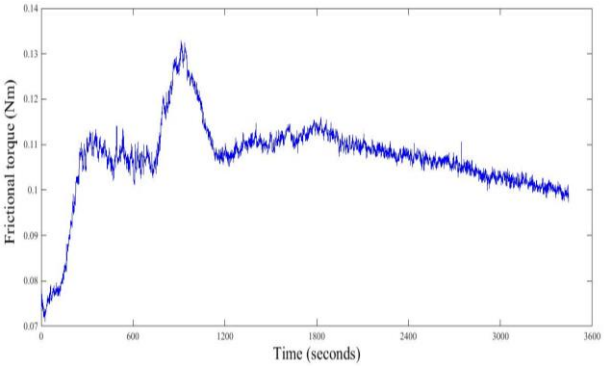

c)

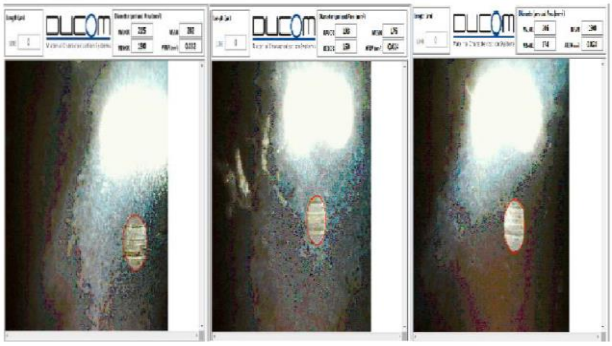

d)

Fig. 10. Friction and wear behavior of MOBIL DTE 25 lubricant : a) Frictional torque without TiO_2 nanoparticles; b) Wear scar view of three balls without TiO_2 nanoparticles; c) Frictional torque with TiO_2 nanoparticles; d) Wear scar view of three balls with TiO_2 nanoparticles

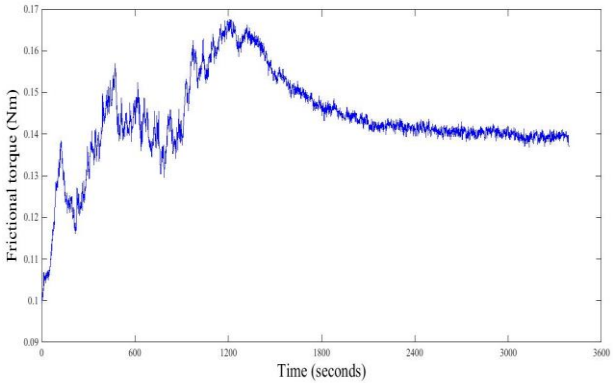

a)

The TiO_2 nanoparticles that are added to the base lubricant, increases the viscosity thereby increases the oil film thickness that reduces the contact between the ball surfaces. The film that is formed is known as tribochemical reaction film and it remained stable during the experimentation that minimized asperity contact [37-38]. After the tests carried out to identify the friction behavior of lubricants with and without nanoparticle, it is clearly observed that the coefficient of friction is reduced for the lubricant operating with TiO_2 nanoparticle additives.

5.2 Comparative analysis of frictional torque of lubricants

The comparative analysis of frictional torque for three grade lubricants with addition of TiO_2 nanoparticles is carried out as shown in Fig. 11. It can be seen that the curve shows a similar trend for all the readings taken on four ball tester.

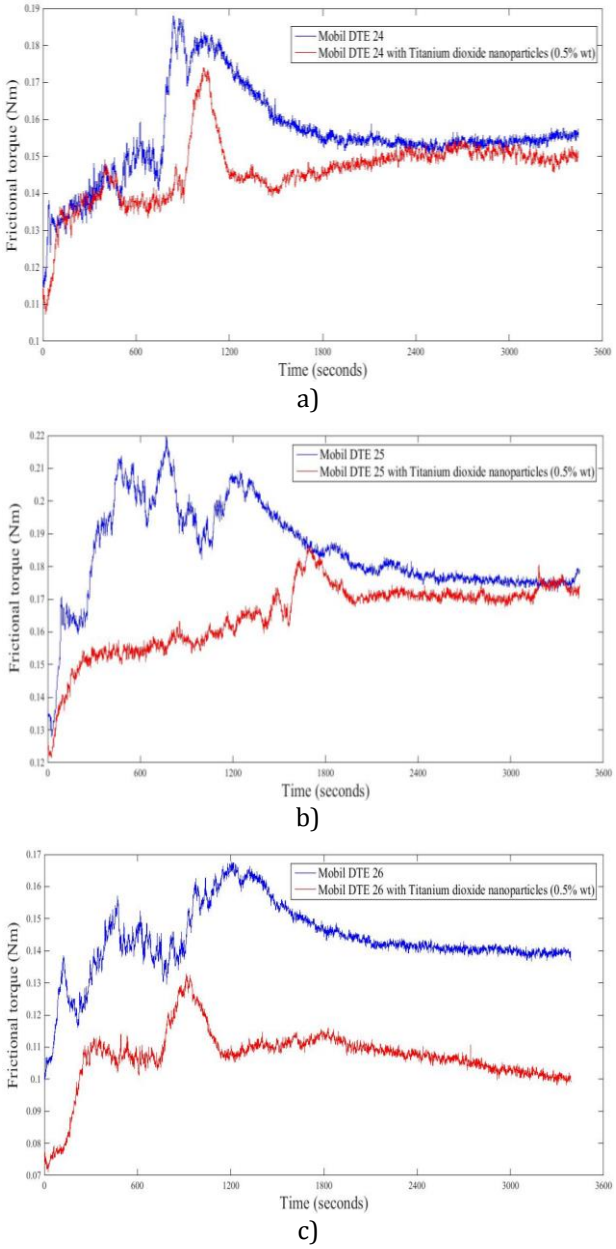

Fig. 11. Influence of TiO_2 nanoparticles (0.5%wt) on frictional torque for: a) MOBIL DTE 24; b) MOBIL DTE 25; c) MOBIL DTE 26.

From Fig. 11, it is observed that the frictional torque for lubricants with TiO_2 nanoparticles is less than the frictional torque for lubricants without TiO_2 nanoparticles. The coefficient of friction for DTE 24, DTE 25 and DTE 26 is reduced by 6.06 %, 7.83 % and 26.36 % respectively, after addition of TiO_2 nanoparticles in the lubricant as shown in Fig. 12.

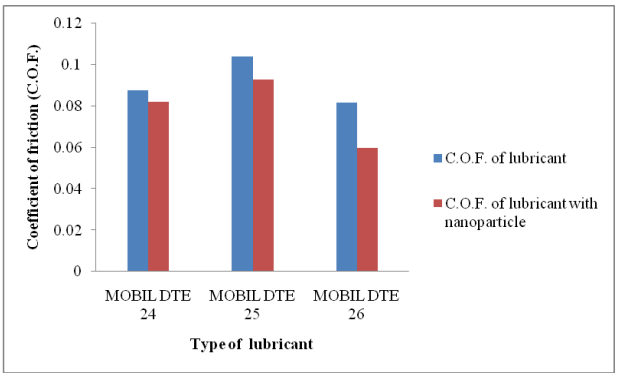

Fig. 12. Comparative analysis of C.O.F. for different lubricants.

However, average frictional coefficient in DTE 25 without TiO_2 nanoparticles is slightly higher than other two oils without TiO_2 nanoparticles due to the formation and variation of formed thin film between the contacting surfaces.

5.3 Comparative analysis of wear scar diameters

The wear scar diameters for lower three balls are measured with the help of a microscope and images are stored using the image acquisition system. The comparison of wear scar diameter in microns is presented in Fig. 13.

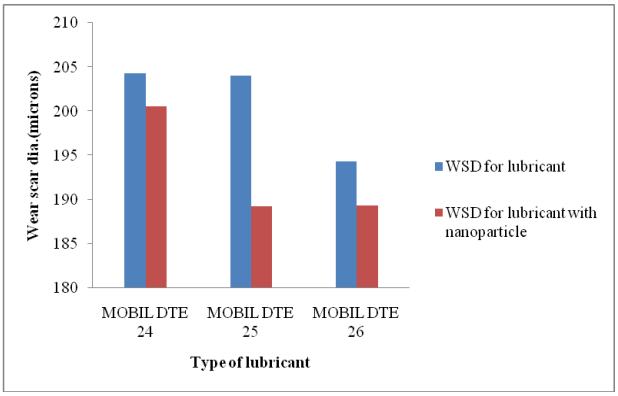

Fig. 13. Comparative analysis of Wear Scar Diameter for different lubricants.

It is clearly seen that the wear scar diameter of lubricant is higher for DTE 24 than DTE 25 and DTE 26. After addition of TiO_2 nanoparticles in the lubricant, the wear scar diameter decreases for DTE 24, DTE 25 and DTE 26 by 1.85 %, 7.20 % and 2.57 % respectively.

6. PERFORMANCE CHARACTERISTICS FOR JOURNAL BEARING

The performance characteristics of plain and elliptical journal bearing are evaluated for three grades of lubricant with TiO_2 nanoparticles. The characteristic number or Sommerfeld number is calculated for various operating conditions and the corresponding eccentricity ratio obtained for the analysis. To identify an influence of TiO_2 nanoparticles as a lubricant additive on the performance characteristics of journal bearing, full factorial design is adopted. Hence for 03 grades of lubricant and 03 various speeds, the total number of experiment are 09 for one set of bearing. The values of dimensionless parameters such as Q/nRCL, Q_s/Q, fR/C are referred from Raimondi Boyd chart [47,48] and intermediate values are estimated using a linear interpolation method. The pressure distribution in the oil film is computed from the Reynold's equation. The eccentricity ratio is calculated for each lubricant at different operating conditions. The pressure distribution using Eq. (4) is computed upto $\theta=\pi$ by considering the cavitation phenomenon [10]. Fig. 14 depicts the variation in pressure distribution in circumferential directions at speeds between 500-1000 rpm and 1 kN load [10]. It is observed that the pressure distribution values in lubricant film are very much higher in elliptical journal bearing than that of plain journal bearing for all types of lubricant. As the speed of journal and viscosity of lubricant increases, the pressure distribution increases for all lubricants. Only in the case of 500 rpm for MOBIL DTE 24 with and without TiO_2 nanoparticles, pressure is lower in elliptical bearing than the plain bearing because the eccentricity ratio is lower than that of plain bearing. The performance characteristics of journal bearing are computed at different operating speeds and lubricants as shown in Table 4. The detailed discussion on each performance characteristic is presented further. The results represented in this section are having similar behavior to the pattern reported by Babu et al. [46].

Table 4. Performance characteristics for journal bearing at different operating speeds.

Type of bearing	Type of lubricant	Viscosity (Mpa-s)	Speed (r.p.m.)	S	ε	Φ (deg.)	W (N)	F_f (N)	f	P_f (Watt)	fR/C	Q/nRCL	Q_s/Q	ΔT (°C)
Plain bearing without TiO_2	MOBIL DTE 24	$2.817*10^{-8}$	500	0.14672	0.5506	56.593	4971.3205	9.6688887	0.0019449	12650.129	3.854	4.24	0.634	4.4184
			750	0.22008	0.4517	63.149	5981.3867	12.430353	0.0020782	24394.568	5.1256	4.0778	0.5443	5.7334
			1000	0.29344	0.375	67.978	6560.78	14.943999	0.0022778	39103.464	6.666	3.94	0.4698	7.3416
	MOBIL DTE 25	$4.063*10^{-8}$	500	0.21161	0.4616	62.511	5886.9331	12.125425	0.0020597	15864.098	5.001	4.094	0.5531	5.6058
			750	0.31742	0.3547	69.227	6702.1063	15.76641	0.0023525	30941.579	7.377	3.899	0.4478	8.0937
			1000	0.42323	0.2835	73.533	7115.7734	19.422916	0.0027296	50823.296	9.873	3.757	0.37	10.705
	MOBIL DTE 26	$5.968*10^{-8}$	500	0.31083	0.3603	68.883	6669.3692	15.544365	0.0023307	20337.211	7.181	3.91	0.453	7.8829
			750	0.46625	0.2663	74.558	7359.3689	21.036821	0.0028585	41284.762	10.476	3.7224	0.3518	11.338
			1000	0.62167	0.2041	78.225	7511.0016	26.577725	0.0035385	69545.046	12.65	3.5982	0.2844	13.607
Plain bearing with TiO_2	MOBIL DTE 24	$2.915*10^{-8}$	500	0.15281	0.5451	56.97	5117.4429	9.9780782	0.0019498	13054.652	3.925	4.236	0.629	4.4876
			750	0.22922	0.4409	63.841	6070.9232	12.748486	0.0020999	25018.903	5.264	4.059	0.5344	5.8756
			1000	0.30563	0.3647	68.613	6639.9539	15.366534	0.0023143	40209.098	7.027	3.919	0.4586	7.7241
	MOBIL DTE 25	$4.207*10^{-8}$	500	0.21526	0.4572	62.795	5926.9254	12.255406	0.0020678	16034.157	5.054	4.087	0.5493	5.6601
			750	0.32289	0.35	69.515	6725.0073	15.947874	0.0023714	31297.704	7.5425	3.89	0.4427	8.2673
			1000	0.43052	0.2806	73.706	7163.5946	19.699846	0.00275	51547.932	9.974	3.751	0.3674	10.815
	MOBIL DTE 26	$6.183*10^{-8}$	500	0.31688	0.3551	69.202	6698.2979	15.746842	0.0023509	20602.118	7.3637	3.9	0.4482	8.0791
			750	0.47531	0.2626	74.778	7397.3847	21.369926	0.0028888	41938.479	10.605	3.7152	0.3479	11.473
			1000	0.63375	0.1997	78.483	7491.5072	27.003943	0.0036046	70660.318	12.84	3.5983	0.2796	13.772
Elliptical bearing without TiO_2	MOBIL DTE 24	$2.817*10^{-8}$	500	0.018	0.9254	89.19	14836.804	28.995009	0.0019543	37935.137	0.855	4.769	0.9385	1.1215
			750	0.0417	0.8112	89.364	13589.863	25.867376	0.0019034	50764.726	1.6272	4.6334	0.8506	2.0288
			1000	0.0672	0.7289	89.463	14601.583	27.545659	0.0018865	72077.809	2.2411	4.5167	0.7843	2.7101
	MOBIL DTE 25	$4.063*10^{-8}$	500	0.0388	0.8223	89.349	13518.376	25.781276	0.0019071	33730.503	1.555	4.646	0.8591	1.9479
			750	0.0738	0.7083	89.485	15061.426	28.400134	0.0018856	55735.262	2.3969	4.487	0.7677	2.8784
			1000	0.1027	0.6409	89.55	17341.993	32.858552	0.0018947	85979.877	2.9099	4.3891	0.713	3.4205
	MOBIL DTE 26	$5.968*10^{-8}$	500	0.072	0.7139	89.479	14939.136	28.170788	0.0018857	36856.781	2.3543	4.4951	0.7722	2.8325
			750	0.1094	0.626	89.564	18512.558	35.167242	0.0018996	69015.712	3.0224	4.3677	0.701	3.5372
			1000	0.1341	0.5773	89.606	22289.008	42.89547	0.0019245	112243.15	3.5116	4.2914	0.6592	4.0524
Elliptical bearing with TiO_2	MOBIL DTE 24	$2.915*10^{-8}$	500	0.018	0.9188	89.201	14800.629	28.871185	0.0019507	37773.133	0.906	4.7614	0.9334	1.1846
			750	0.0448	0.7992	89.379	13667.265	25.964787	0.0018998	50955.895	1.706	4.6188	0.8413	2.1166
			1000	0.0706	0.7183	89.474	14839.848	27.985761	0.0018859	73229.407	2.3209	4.5015	0.7758	2.7965
	MOBIL DTE 25	$4.207*10^{-8}$	500	0.0401	0.8174	89.356	13542.226	25.803962	0.0019054	33760.184	1.5869	4.6408	0.8553	1.9835
			750	0.0753	0.7036	89.49	15159.411	28.585221	0.0018856	56098.496	2.4326	4.4802	0.7639	2.9167
			1000	0.1039	0.6383	89.553	17545.608	33.257644	0.0018955	87024.168	2.9289	4.3855	0.711	3.4403
	MOBIL DTE 26	$6.183*10^{-8}$	500	0.0737	0.7087	89.484	15049.146	28.37701	0.0018856	37126.588	2.3938	4.4876	0.768	2.875
			750	0.1108	0.6228	89.567	18748.442	35.637468	0.0019008	69938.531	3.0467	4.363	0.6984	3.5623
			1000	0.1359	0.5742	89.609	22575.183	43.493415	0.0019266	113807.77	3.5515	4.2861	0.6563	4.0946

The eccentricity ratio is widely increased in elliptical bearing than plain bearing as the speed increases. Nevertheless it also be noted that, due to addition of TiO_2 nanoparticles, the pressure distribution is increased significantly for both the bearings as shown in Fig. 14.

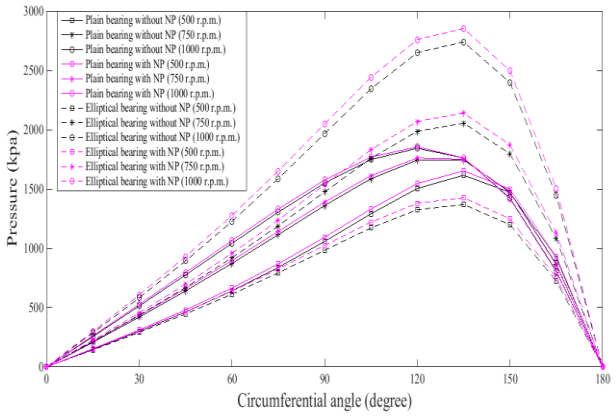

a)

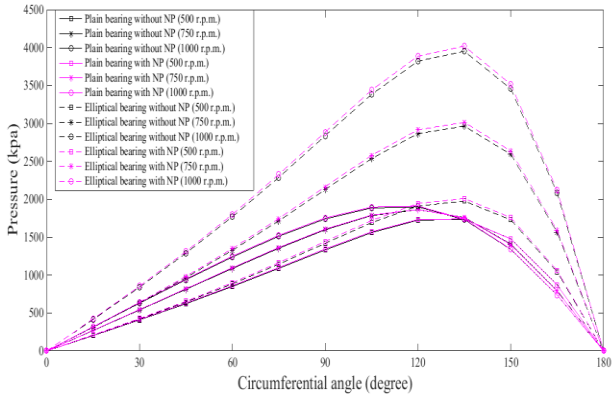

b)

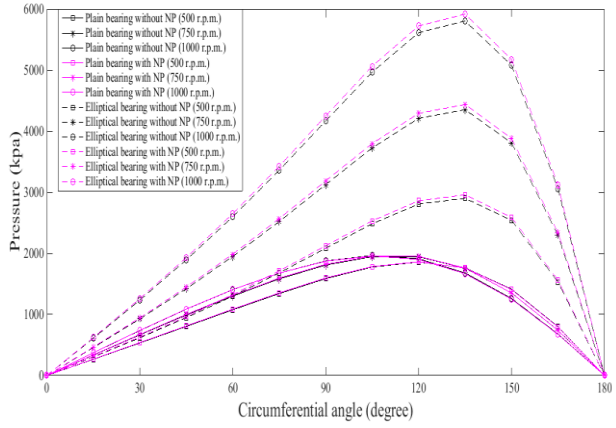

c)

Fig. 14. Variation in pressure distribution in circumferential direction at various speeds: a) MOBIL DTE 24; b) MOBIL DTE 25; c) MOBIL DTE 26.

Figure 15 represents the comparative analysis of plain and elliptical bearing for attitude angle considering selected lubricants with the addition of the TiO_2 nanoparticles. From the computation using Eq. (10), it has been observed that the attitude angle increases in the loaded lobe of an elliptical journal bearing significantly by 15.48 % to 59.37 % than a plain journal bearing. It is the angle at which the maximum pressure distribution can be identified. TiO_2 nanoparticles in the lubricant influence the value of attitude angle and attitude angle increases by 0.23 % to 1.10 % as shown in Fig. 15.

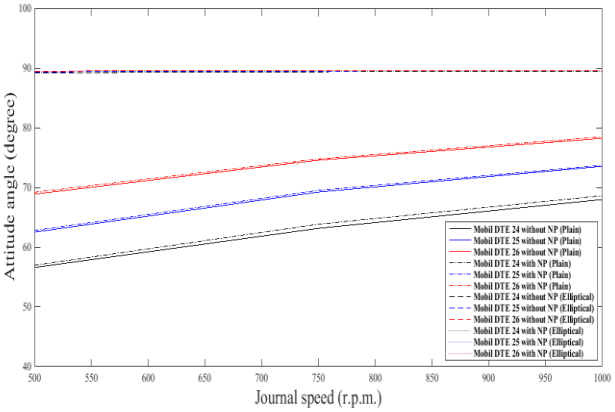

Fig. 15. Variation in attitude angle with and without nanoparticles (TiO_2) in the lubricant.

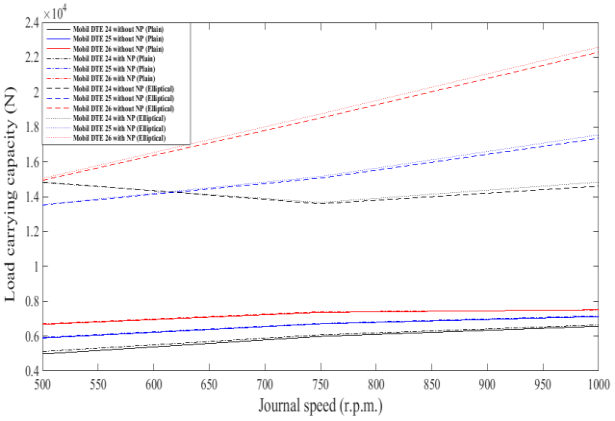

Fig. 16. Variation in load carrying capacity with and without nanoparticles (TiO_2) in the lubricant.

The comparative analysis of plain and elliptical bearing for load carrying capacity considering selected lubricants with the addition of the nanoparticle is demonstrated in Fig. 16. The Eq. (14) is used to estimate the load carrying capacity at different operating conditions for various grades of lubricant. It is interesting to note that the load carrying capacity of an elliptical journal bearing increases significantly by 2.24 to 3.01 times than a plain journal bearing. It is also observed that as the viscosity of oil increases due to addition of TiO_2 nanoparticles, load carrying capacity increases by 0.34 % to 2.93 % in both the bearings. A

combined influence of bearing configuration and lubricant additives enhance the load carrying capacity of journal bearing appreciably.

The Eq. (20) has been implemented to calculate the frictional force in the bearings. Figure 17 illustrates the comparative analysis of plain and elliptical bearing operating with and without nanolubricant for frictional force. It is observed that the frictional force increases in elliptical journal bearing than plain journal bearing due to an increase in eccentricity ratio. It is also noted that for MOBIL DTE 24 lubricant, the elliptical bearing achieved a slight decrease in frictional force. The frictional coefficient gets reduced in the elliptical bearing as per the Eq. (21).

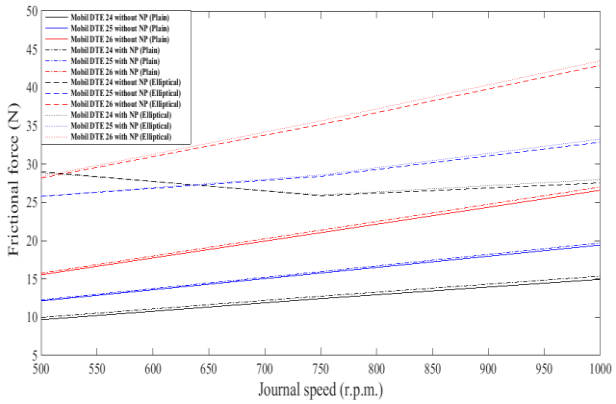

Fig. 17. Variation in frictional force with and without nanoparticles (TiO_2) in the lubricant.

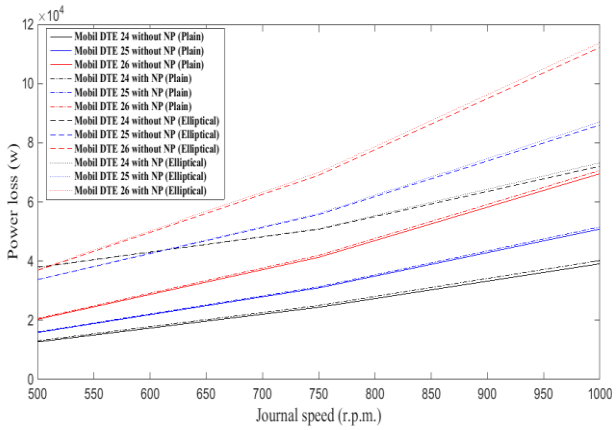

Fig. 18. Variation in power loss with and without nanoparticles (TiO_2) in the lubricant.

The power loss due to the friction is computed using Eq. (23). Fig. 18 depicts the comparative analysis of plain and elliptic bearing for power loss due to friction considering selected lubricants with the addition of the TiO_2 nanoparticles. It is observed that power loss also increases in the lower lobe of an elliptical journal bearing than plain journal bearing due to an additional clearance in the bearing surface.

The dimensionless parameters like Q/nRCL, Q_s/Q and fR/C are referred from the Raimondi Boyd chart. The values of these dimensionless parameters for the various intermediate eccentricity ratio are computed using a linear interpolation technique. The sample calculation of eccentricity ratio 0.5 is mentioned in the Table 4 to compute the dimensionless parameters. Figure 19 represents the comparative analysis of plain and elliptical bearing for the flow rate ratio to determine the oil flow rate considering selected lubricants with the addition of the TiO_2 nanoparticle additives. It is noticed that the flow rate ratio increases in elliptical journal bearing than plain journal bearing for same operating conditions due to increase in eccentricity. From the obtained value of oil flow rate ratio, the oil flow rate is computed by considering the geometrical values for bearing. The oil flow rate falls in both the bearings after addition of TiO_2 nanoparticles. In plain bearing, the oil flow rate is decreased upto 0.53 % while in elliptical bearing the oil flow rate is decreased upto 0.33 %. This indicates that the TiO_2 nanoparticle additives influence the oil flow rate for the bearing that will minimize the oil consumption.

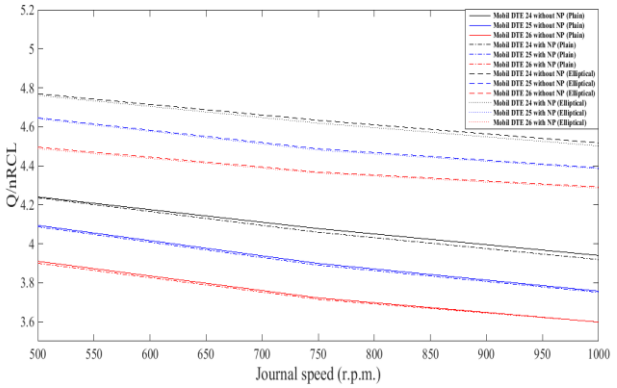

Fig. 19. Variation in oil flow rate with and without nanoparticles (TiO_2) in the lubricant.

In the similar way, the ratio of side leakage to oil flow rate is determined from the corresponding eccentricity ratio. The comparison of side leakage through plain and elliptical bearing for different lubricating conditions is depicted in Fig. 20. It is observed that the side flow increases in elliptical journal bearing than plain journal bearing for same operating conditions due to increase in eccentricity ratio and oil flow rate. However, the side leakage is decreased in both

the bearings after addition of TiO_2 nanoparticles. The ratio of friction coefficient variable (dimensionless) for plain and elliptical bearing is represented in Fig. 21 operating with different lubricants. From the comparison as shown in Fig. 21, it is observed that the coefficient of friction decreases remarkably in elliptical journal bearing than plain journal bearing for same operating conditions. It is very desirable from performance perspectives of bearing. The coefficient of friction gets reduced from 67.7 % to 77.81 % in the elliptical journal bearing.

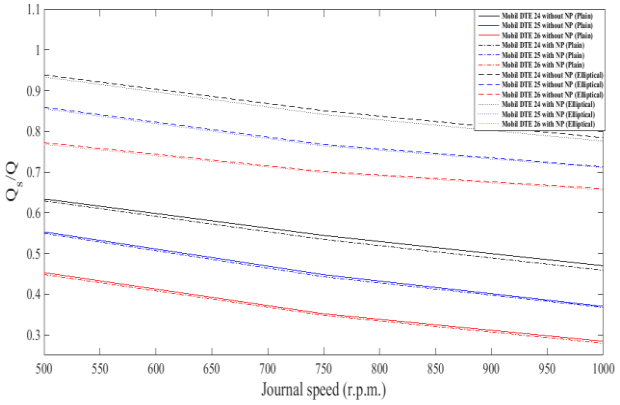

Fig. 20. Variation in side leakage flow with and without nanoparticles(TiO_2) in the lubricant.

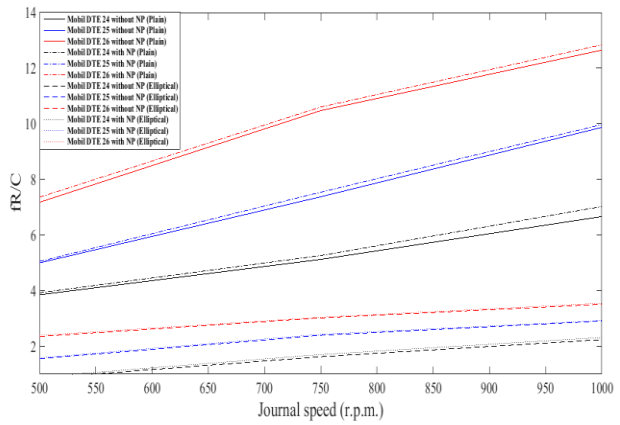

Fig. 21. Variation in frictional coefficient with and without nanoparticles(TiO_2) in the lubricant.

After addition of TiO_2 nanoparticle additives in the lubricant, the coefficient of friction is slightly increased in both the bearings due to increase in frictional force.

The aspect regarding the temperature rise in a fluid film is also analyzed. The temperature rise in a journal bearing affects the lubricant properties and performance of the system. For the selected lubricants operating with and without TiO_2 nanoparticle additives, the comparison of temperature rise in a fluid film is illustrated in Fig. 22 for plain and elliptical bearing.

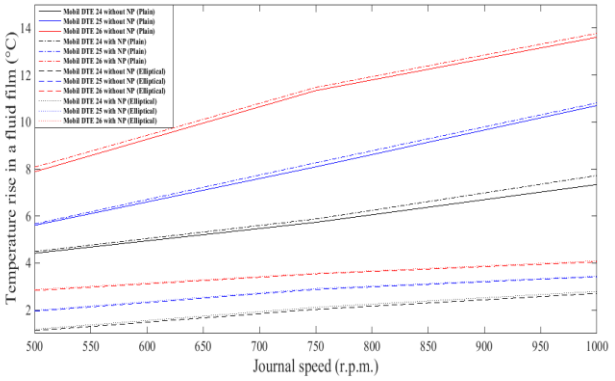

Fig. 22. Variation in temperature rise with and without nanoparticles (TiO_2) in the lubricant.

It is observed that the temperature rise in the loaded lobe of elliptical journal bearing is very much lower than that of plain journal bearing for same operating conditions. The temperature rise is decreased from 63.07 % to 74.60 % in an elliptical bearing as compared to plain bearing.

7. CONCLUSION

The plain and elliptical journal bearings operating with TiO_2 nanoparticle based lubricant are considered in this research study. An analytical approach is presented to evaluate the performance characteristics at different operating conditions. TiO_2 nanoparticles (0.5%wt) are added in the lubricants to analyze the performance of bearings. Four ball tribo-tester is used to analyze the lubricant performance. The various performance characteristics of plain as well as elliptical journal bearing are evaluated.

The following conclusions have been drawn from the present study:

- The anti-friction and anti-wear properties are improved for the lubricants operating with TiO_2 nanoparticle additives. For the selected MOBIL grade lubricants containing TiO_2 nanoparticles, the frictional coefficient for DTE 26 is reduced as a maximum while wear scar diameter measured for the steel balls are reduced for DTE 25 as a maximum.
- The performance characteristics are improved using elliptical bearing over plain bearing. The performance parameters such

as pressure distribution, frictional force, maximum pressure built up are increased in the elliptical bearing. Along with this, attitude angle is increased by 15.48 % to 59.37 % and load carrying capacity is increased significantly by 2.24 to 3.01 times than that of plain bearing. It has been also observed that the temperature rise is reduced by 63.07 % to 74.60 % and frictional coefficient by 67.7 % to 77.81 % in the elliptical bearing. However, power loss, oil flow rate and side leakage are increased upto certain extent due to an additional clearance available in the elliptical bearing.

- After addition of TiO_2 nanoparticles in the lubricant, the viscosity of the lubricant is increased. It tends to increase the pressure distribution, frictional force, attitude angle by 0.23 % to 1.10 %, load carrying capacity by 0.34 % to 2.93 % while the oil flow rate is reduced by 0.33 % to 0.53 % along with side leakage.
- An elliptical bearing operating with nanolubricant shows the superior performance over other combinations.

Acknowledgement

The author would wish to convey his sincere gratitude to his parents, Dr. J. T. Pattiwar, Dr. V. P. Wani, Dr. A. G. Thakur, colleagues, friends for their kind cooperation, motivation and support during the study. This study is supported by Research Scheme under B.C.U.D. (Board of College and University Department), Savitribai Phule Pune University, Pune, India.

REFERENCES

[1] N. Ram, S.C. Sharma, *Analysis of orifice compensated non-recessed hole-entry hybrid journal bearing operating with micro polar lubricants*, Tribology International, vol. 52, pp. 132-143, 2012, doi: 10.1016/j.triboint.2012.03.012

[2] Q. Lin, Z.Y. Wei, N. Wang, W. Chen, *Analysis on the lubrication performances of journal bearing system using computational fluid dynamics and fluid–structure interaction considering thermal influence and cavitation*, Tribology International, vol. 64, pp. 8-15, 2013, doi: 10.1016/j.triboint.2013.03.001

[3] K.P. Gertzos, P.G. Nikolakopoulos, C.A. Papadopoulos, *CFD analysis of journal bearing hydrodynamic lubrication by Bingham lubricant*, Tribology International, vol. 41, iss. 12, pp. 1190-1204, 2008, doi: 10.1016/j.triboint.2008.03.002

[4] M. Deligant, P. Podevin, G. Descombes, *CFD model for turbocharger journal bearing performances*, Applied Thermal Engineering, vol. 31, iss. 5, pp. 811-819, 2011, doi: 10.1016/j.applthermaleng.2010.10.030

[5] D.A. Bompos, P.G. Nikolakopoulos, *CFD simulation of magneto rheological fluid journal bearings*, Simulation Modelling Practice and Theory, vol. 19, iss. 4, pp. 1035-1060, 2011, doi: 10.1016/j.simpat.2011.01.001

[6] A. Chasalevris, D. Sfyris, *Evaluation of the finite journal bearing characteristics, using the exact analytical solution of the Reynolds equation*, Tribology International, vol. 57, pp. 216-234, 2013, doi: 10.1016/j.triboint.2012.08.011

[7] F.P. Brito, A.S. Miranda, J.C.P. Claro, M. Fillon, *Experimental comparison of the performance of a journal bearing with a single and a twin axial groove configuration*, Tribology International, vol. 54, pp. 1-8, 2012, doi: 10.1016/j.triboint.2012.04.026

[8] C.A. Papadopoulos, P.G. Nikolakopoulos, G.D. Gounaris, *Identification of clearances and stability analysis for a rotor-journal bearing system*, Mechanism and Machine Theory, vol. 43, iss. 4, pp. 411-426, 2008, doi: 10.1016/j.mechmachtheory.2007.04.007

[9] S.C. Sharma, N. Ram, *Influence of micropolar lubricants on the performance of slot-entry hybrid journal bearing*, Tribology International, vol. 44, iss. 12, pp. 1852-1863, 2011, doi: 10.1016/j.triboint.2011.07.006

[10] D.Y. Dhande, D.W. Pande, *Multiphase flow analysis of hydrodynamic journal bearing using CFD coupled Fluid Structure Interaction considering cavitation*, Journal of King Saud University - Engineering Sciences, in press, 2016, doi: 10.1016/j.jksues.2016.09.001

[11] H. Montazeri, *Numerical analysis of hydrodynamic journal bearings lubricated with ferrofluid*, Engineering Tribology, vol. 222, iss. 1, pp. 51-60, 2008, doi: 10.1243/13506501JET314

[12] A. Ouadoud, A. Mouchtachi, N. Boutammachte, *Numerical simulation CFD, FSI of a hydrodynamic journal bearing*, Journal of Advanced Research in Mechanical Engineering, vol. 2, iss. 1, pp. 33-38, 2011.

[13] K.G. Binu, K. Yathish, R. Mallya, B.S. Shenoy, D.S. Rao, R. Pai, *Experimental study of hydrodynamic*

pressure distribution in oil lubricated two-axial groove journal bearing, Materials Today: Proceedings, vol. 2, iss. 4-5, pp. 3453-3462, 2015, doi: 10.1016/j.matpr.2015.07.321

[14] S. Boubendir, S. Larbi, R. Bennacer, *Numerical study of the thermo-hydrodynamic lubrication phenomena in porous journal bearings*, Tribology International, vol. 44, iss. 1, pp. 1-8, 2011, doi: 10.1016/j.triboint.2010.09.008

[15] E.R. Nicodemus, S.C. Sharma, *Orifice compensated multirecess hydrostatic/hybrid journal bearing system of various geometric shapes of recess operating with micropolar lubricant*, Tribology International, vol. 44, iss. 3, pp. 284-296, 2011, doi: 10.1016/j.triboint.2010.10.026

[16] A.D. Rahmatabadi, M. ZareMehrjardi, M.R. Fazel, *Performance analysis of micropolar lubricated journal bearings using GDQ method*, Tribology International, vol. 43, iss. 11, pp. 2000-2009, 2010, doi: 10.1016/j.triboint.2010.05.002

[17] H.C. Garg, VijayKumar, H.B. Sharda, *Performance of slot-entry hybrid journal bearings considering combined influences of thermal effects and non-Newtonian behavior of lubricant*, Tribology International, vol. 43, iss. 8, pp. 1518-1531, 2010, doi: 10.1016/j.triboint.2010.02.013

[18] A. Cristea, J. Bouyer, M. Fillon, M.D. Pascovici, *Transient Pressure and Temperature Field Measurements in a Lightly Loaded Circumferential Groove Journal Bearing from Startup to Steady-State Thermal Stabilization*, Tribology Transactions, vol. 60, iss. 6, pp. 988-1010, 2017, doi: 10.1080/10402004.2016.1241330

[19] M. Mongkolwongrojn, C. Aiumpronsins, *Stability analysis of rough journal bearings under TEHL with non-Newtonian lubricants*, Tribology International, vol. 43, iss. 5-6, pp. 1027-1034, 2010, doi: 10.1016/j.triboint.2009.12.039

[20] K.P. Nair, V.P. Sukumaran Nair, N.H. Jayadas, *Static and dynamic analysis of elastohydrodynamic elliptical journal bearing with micropolar lubricant*, Tribology International, vol. 40, iss. 2, pp. 297-305, 2007, doi: 10.1016/j.triboint.2005.09.017

[21] S.C. Sharma, V. Kumar, S.C. Jain, T. Nagaraju, *Study of hole-entry hybrid journal bearing system considering combined influence of thermal and elastic effects*, Tribology International, vol. 36, iss. 12, pp. 903-920, 2003, doi: 10.1016/S0301-679X(03)00074-4

[22] N.M. Ene, F. Dimofte, T.G. Keith, *A stability analysis for a hydrodynamic three-wave journal bearing*, Tribology International, vol. 41, iss. 5, pp. 434-442, 2008, doi: 10.1016/j.triboint.2007.10.002

[23] P.C. Mishra, R.K. Pandey, K. Athre, *Temperature profile of an elliptic bore journal bearing*, Tribology International, vol. 40, iss. 3, pp. 453-458, 2007, doi: 10.1016/j.triboint.2006.04.009

[24] E. Kuznetsov, S. Glavatskih, M. Fillon, *THD analysis of compliant journal bearings considering liner deformation*, Tribology International, vol. 44, iss. 12, pp. 1629-1641, 2011, doi: 1016/j.triboint.2011.05.013

[25] F.P. Brito, A.S. Miranda, J.C.P. Claro, J.C. Teixeira, L. Costa, M. Fillon, *The role of lubricant feeding conditions on the performance improvement and friction reduction of journal bearings*, Tribology International, vol. 72, pp. 65-82, 2014, doi: 10.1016/j.triboint.2013.11.016

[26] W.M. Miranda, M.T.C. Faria, *Lateral Vibration Analysis of Flexible Shafts Supported on Elliptical Journal Bearings*, Tribology Letters, vol. 48, iss. 2, pp. 217-227, 2012, doi: 10.1007/s11249-012-0018-5

[27] X.-L. Wang, K.-Q. Zhu, S.-Z. Wen, *Thermohydrodynamic analysis of journal bearings lubricated with couple stress fluids*, Tribology International, vol. 34, iss. 5, pp. 335-343, 2001, doi: 10.1016/S0301-679X(01)00022-6

[28] R. Sehgal, *Experimental Measurement of Oil Film Temperatures of Elliptical Journal Bearing Profile Using Different Grade Oils*, Tribology Online, vol. 5, iss. 6, pp. 291-299, 2010, doi: 10.2474/trol.5.291

[29] K.G. Binu, B.S. Shenoy, D.S. Rao, R. Pai R, *A Variable Viscosity Approach for the Evaluation of Load Carrying Capacity of Oil Lubricated Journal Bearing with TiO_2 Nanoparticles as Lubricant Additives*, Procedia Materials Science, vol. 6, pp. 1051-1067, 2014, doi: 10.1016/j.mspro.2014.07.176

[30] S. Baskar, G. Sriram, S. Arumugam, *Experimental analysis on tribological behavior of nano based bio-lubricants using four ball tribometer*, Tribology in Industry, vol. 37, no. 4, pp. 449-454, 2015.

[31] K. Hu, Y. Cai, X. Hu, Y. Xu, *Synergistic lubrication of MoS_2 particles with different morphologies in liquid paraffin*, Industrial Lubrication and Tribology, vol. 65, iss. 3, pp. 143-149, 2013, doi: 10.1108/00368791311311141

[32] S. Baskar, G. Sriram, *Tribological behavior of journal bearing material under different lubricants*, Tribology in Industry, vol. 36, no. 2, pp. 127-133, 2014.

[33] Q. Wan, Y. Jin, P. Sun, Y. Ding, *The Tribological behavior of a lubricant oil containing boron nitride nanoparticles*, Procedia Engineering, vol. 102, pp. 1038-1045, 2015, doi: 10.1016/j.proeng.2015.01.226

[34] F. Ilie, C. Covaliu, *Tribological Properties of the Lubricant Containing Titanium Dioxide Nanoparticles as an Additive,* Lubricants, vol. 4, pp. 1-13, 2016, doi: 10.3390/lubricants4020012

[35] M. S. Charoo, M. F. Wani, *Tribological properties of IF- MoS_2 nanoparticles as lubricant additive on cylinder liner and piston ring tribo-pair*, Tribology in Industry, vol. 38, no. 2, pp. 156-162, 2016.

[36] M. Laad, V.K.S. Jatti, *Titanium oxide nanoparticles as additives in engine oil*, Journal of King Saud University - Engineering Sciences, vol. 30, iss. 2, pp. 116-122, 2016, doi: 10.1016/j.jksues.2016.01.008

[37] M.K.A. Ali, P. Fuming, H.A. Younus, M.A.A. Abdelkareem, F.A. Essa, A. Elagouz, H. Xianjun, *Fuel economy in gasoline engines using Al_2O_3/TiO_2 nanomaterials as nanolubricant additives*, Applied Energy, vol. 211, pp. 461-478, 2018, doi: 10.1016/j.apenergy.2017.11.013

[38] M.K.A. Ali, H. Xianjun, A. Elagouz, F.A. Essa, M.A. A. Abdelkareem, *Minimizing of the boundary friction coefficient in automotive engines using Al_2O_3 and TiO_2 nanoparticles*, Journal of Nanoparticle Research, vol. 18, pp. 1-16, 2016, doi: 10.1007/s11051-016-3679-4

[39] M.K.A. Ali, H. Xianjun, L. Mai, C. Bicheng, R.F. Turkson, C. Qingping, *Reducing frictional power losses and improving the scuffing resistance in automotive engines using hybrid nanomaterials as nano-lubricant additives*, Wear, vol. 364-365, pp. 270-281, 2016, doi: 10.1016/j.wear.2016.08.005

[40] W. Gunnuang, C. Aiumpornsin, M. Mongkolwongrojn, *Effect of Nanoparticle Additives on Journal Bearing Lubricated with Non-Newtonian Carreau Fluid*, Applied Mechanics and Materials, vol. 751, pp. 137-142, 2015, doi: 10.4028/www.scientific.net/AMM.751.137

[41] A.A. Solghar, *Investigation of nanoparticle additive impacts on thermohydrodynamic characteristics of journal bearings*, Proceedings of the Institution of Mechanical Engineers, Part J: Journal of Engineering Tribology, vol. 229, iss. 10, pp. 1176-1186, 2015, doi: 10.1177/1350650115574734

[42] B.S. Shenoy, K.G. Binu, R. Pai, D.S. Rao, R.S. Pai, *Effect of nanoparticles additives on the performance of an externally adjustable fluid film bearing*, Tribology International, vol. 45, iss. 1, pp. 38-42, 2012, doi: 10.1016/j.triboint.2011.10.004

[43] R. Nicoletti, *The Importance of the Heat Capacity of Lubricants With Nanoparticles in the Static Behavior of Journal Bearings*, Journal of Tribology, vol. 136, iss. 4, pp. 1-5, 2014, doi: 10.1115/1.4027861

[44] W.H. Azmi, K.V. Sharma, P.K. Sarma, R. Mamat, S. Anuar, V.D. Rao, *Experimental determination of turbulent forced convection heat transfer and friction factor with SiO_2 nanofluid*, Experimental Thermal and Fluid Science, vol. 51, pp. 103-111, 2013, doi: 10.1016/j.expthermflusci.2013.07.006

[45] L.S. Khuong, H.H. Masjuk, N.W.M. Zulki, E.N. Mohamad, M.A. Kalam, A. Alabdulkarem, A. Arslan, M.H. Mosarof, A.Z. Syahir, M. Jamshaid, *Effect of gasoline–bioethanol blends on the properties and lubrication characteristics of commercial engine oil*, RSC Advances, vol. 7, iss. 25, pp. 15005-15019, 2017, doi: 10.1039/C7RA00357A

[46] K.S. Babu, K.P. Nair, P.K. Rajendrakumar, *Computational analysis of journal bearing operating under lubricant containing Al_2O_3 and ZnO nanoparticles*, International Journal of Engineering, Science and Technology, vol. 6, no. 1, pp. 34-42, 2014.

[47] H. Avraham, *Bearing Design in Machinery*, New York: Marcel Dekker Inc., 2002.

[48] D.D. Fuller, *Theory and practice of lubrication for engineers*, New York: Wiley, 1984.

[49] Manganese (Mn) Nanoparticles - Properties, Applications at https://www.azonano.com/article.aspx?ArticleID=3291

[50] Zinc Nanoparticles at https://www.americanelements.com/zinc-nanoparticles-7440-66-6

Nomenclature

g Acceleration due to gravity, m/s^2

W_b Applied load on balls, N

f Bearing frictional coefficient

W_X Bearing load carrying capacity in X direction, N

W_Y Bearing load carrying capacity in Y direction, N

P Bearing pressure, kPa

D Diameter of journal, mm

C Diametrical clearance, mm

r Distance measured from the center of the lower ball contact surface to the rotating axis, m

e Eccentricity, mm

E_m Elliptical ratio

F External load acting on shaft, N

h_o Film thickness at the point of peak pressure, mm

D Fractional index

F_f Frictional force, N

T_f Frictional torque, Nm

Q Flow rate, m^3/s

C_h Horizontal clearance for elliptical journal bearing, mm
U Journal surface velocity, m/s
L Length of bearing, mm
W Load carrying capacity, N
C_m Minimum clearance when the center of shaft coincides with the center of elliptic bearing, mm
h_m Minimum oil film thickness, mm
h Oil variable film thickness, mm
p Pressure on fluid film, kPa
P_f Power loss per unit time, Watt
W_{bf} Quantity of base fluid, ml
c Radial clearance, mm
a_a Radius of aggregate nanoparticles, nm
R Radius of journal, mm
R_L Radius of lower lobe for elliptical bearing, mm
a Radius of primary nanoparticles, nm
R_U Radius of upper lobe for elliptical bearing, mm
N Rotational speed of journal, r.p.m.
n Rotational speed of journal, r.p.s.
Q_s Side flow rate, m^3/s
S Sommerfeld number
ΔT Temperature rise in a film, degree Celsius
W_{TiO_2} Weight of titanium dioxide nanoparticles, gm

Greek symbols

θ Angular coordinates, degree
ω Angular velocity, rad/sec
ø Attitude angle, degree
$ø_2$ Attitude angle of lower lobe for elliptical bearing, degree
$ø_1$ Attitude angle of upper lobe for elliptical bearing, degree
ρ_{bf} Density of base fluid, kg/m^3
ρ_{TiO_2} Density of titanium dioxide nanoparticles, kg/m^3
μ Dynamic viscosity, MPa-s
ϕ_a Effective volume fraction
ϵ Eccentricity ratio
$\in_2$ Eccentricity ratio at lower lobe for elliptical Bearing
$\in_1$ Eccentricity ratio at upper lobe for elliptical Bearing
μ_b Frictional coefficient between balls and Lubricant
ϕ_m Maximum particle packing fraction
τ Shear stress, N/m^2
γ Sommerfeld variable
μ_{ps} Viscosity of nanofluid, Mpa-s
μ_{bf} Viscosity of base fluid, Mpa-s
ϕ' Volume concentration of nanoparticles

Abbreviation

AC Alternating Current
ADI Alternating Direction Implicit
ASTM American Society for Testing and Materials
CMRO Chemically Modified Rapeseed Oil
COC Cleveland Open Cup
COF Coefficient of Friction
CFD Computational Fluid Dynamics
FEM Finite Element Method
FFT Fast Fourier Transform
FSI Fluid Structure Interaction
GDQ Generalized Differential Quadrature
hp Horse power
IS International Standards
max Maximum
NC Numerically Controlled
NP Nanoparticle
psi Pound per square inch
PTFE Polytetrafluoroethylene
SEM Scanning Electron Microscope
UV Ultra Violet
VFD Variable Frequency Drive
WSD Wear Scar Diameter
XRD X-Ray Diffraction